A Novel Optimization Method for Lenticular 3-D Display Based on Light Field Decomposion

Renjing Pei, Zheng Geng, Zhao Xing Zhang, Xuan Cao, and Rong Wang

***Abstract*—Crosstalk is a primary defect in affecting the image quality of stereoscopic three-dimensional (3-D) displays. Until now, the crosstalk reduction methods either require extra devices or need tedious calibration procedures, which require precise measurement on each display device. We propose herein a new method of synthesizing lenticular 3-D display based on the light field decomposition and optimization to minimize the crosstalk. The light field concept is introduced into lenticular 3-D display. Rays of multiview light field are back-projected to the LCD plane to form a synthetic image, with subpixel resolution. A weighted value considering all arriving rays is assigned for the subpixel to reduce crosstalk. We developed a new algorithm of ray's mergence and assignment for a smooth fusion of different views and crosstalk reduction. We also performed validation experiments which convincingly demonstrated that our new method is capable of reducing the crosstalk on synthetic graph. Compared with existing methods, our proposed new method is simple and effective, and implementation cost is low.**

***Index Terms*—Crosstalk reduction, lenticular 3-D display, light field.**

I. INTRODUCTION

THREE-DIMENSIONAL (3-D) display technologies have attracted considerable research activities for decades with various means to produce high fidelity 3-D scenes. The lenticular 3-D display technology, based on lenticular sheet overlaid onto spatial light modulator (SLM) screen, is relatively simple to implement and its quality of 3-D image reconstruction appears adequate. Significant research efforts over past decades has resulted in numerous commercial products and applications, such as 3D-TV.

One of the key elements of lenticular 3-D display is the mapping, i.e., synthesizing appropriate contents on 2-D SLM based on the desirable 3-D display effect. Mapping accuracy determines the quality of 3-D display. There are various techniques to implement a "perfect" 3-D display [1]. Determining how to perform an accurate 3-D image mapping from multiview image sources is the key to developing lenticular 3-D display techniques. A universal mapping rule is the most popular approach for a simple and speedy algorithm [2]. This rule determines the view number of a given point in the LCD plane by Philips' method [3]. The implementation is relatively simple and the cost is low. However, this method often generates a synthetic map with quite poor imaging quality and crosstalk.

In this article, we introduce the light field concept into the mapping design for lenticular 3-D display. The light field, proposed by Levoy and Hanrahan [4], completely characterizes the radiance flowing through all the points in each possible direction. The ultimate goal of 3-D display systems is to reproduce the light field that is generated by real-world physical objects. The light field display developed by Jones *et al.* [5] consists of a high-speed image projector, a spinning mirror covered by a holographic diffuser, and electronics to decode specially encoded Digital Visual Interface video signals. Wetzstein *et al.* [6] developed tomographic technique for image synthesis on displays, which was composed of compact volumes of light-attenuating material. The target light field was recreated with the optimal multiple-layer decomposition when it was illuminated by a backlight. Wetzstein *et al.* [7] introduced the tensor displays in which a family of compressive light field displayed. The light fields are generated by a stack of light-attenuating LCD layers illuminated by uniform or directional backlighting. Cao *et al.* [8] further improved the optimization technique for light field multilayer 3-D display.

The ultimate purpose for us to introduce the light field technique into synthesizing of the mapping for lenticular 3-D displays is to reduce crosstalk. The crosstalk is a critical defect affecting the image quality in multiview lenticular 3-D display [9]. The incomplete isolation of image channels convey to the left and right eye so that the content from one channel is partly presented in another channel [10]. Various methods have been proposed to reduce crosstalk [11]–[19]. Examples include (1) decreasing the parallax values of the disparity images; (2) lowing aperture ratio in parallax barrier type display; (3) adding pixel mask on lenticular type display [20][21]; (4) timing control of the display panel. All these methods require extra devices, which increases the cost or the power consumption increases.

A common crosstalk coefficients calculation method [11], [22] was proposed to reduce the crosstalk by correcting the values of subpixels in the synthetic images for a 3-D display. The proportions of the received light from the corresponding

Manuscript received December 14, 2015; revised January 03, 2016; accepted January 10, 2016. Date of publication January 12, 2016; date of current version June 15, 2016. This work was supported in part by the National High-tech R&D Program (863 Program) of Institute of Automation, Chinese Academy of Sciences (CASIA) under Grant 2015AA015905.

The authors are with the State Key Laboratory of Management and Control for Complex Systems Institute of Automation, Chinese Academy of Sciences, Beijing 100190, China (e-mail: peirenjing2013@ia.ac.cn; geng.zheng@ia.ac.cn; agilesargentees@gmail.com; caoxuan2012@ia.ac.cn; wangrong2013@ia.ac.cn).

Color versions of one or more of the figures in this paper are available online at http://ieeexplore.ieee.org.

Digital Object Identifier 10.1109/JDT.2016.2517243

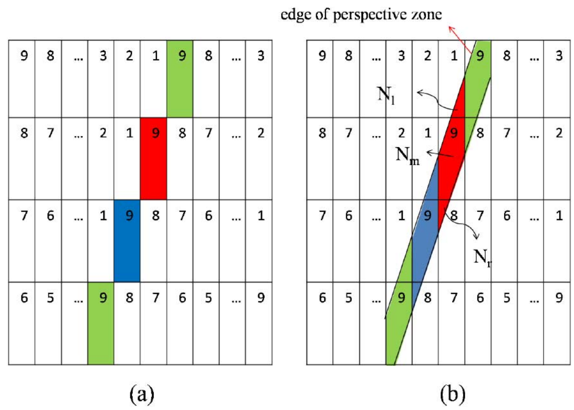

Fig. 1. Distribution mode of nine different parallax images' subpixels on the synthetic image. (a) Ninth view image prepared to display. (b) Ninth view image observed through the lenticular sheet.

view image, its left neighboring view image, and its right neighboring view image are c_m, c_l and c_r, respectively. They are defined as the crosstalk coefficients, with a constraint:

$$c_m + c_l + c_r = 1$$

N_m denotes the viewable area of subpixel belonging to the intended view image and N_l and N_r denote the viewable areas of neighboring unintended subpixel left and right respectively. The distributions of N_m, N_l and N_r are illustrated in Fig. 1. Then, c_m, c_l and c_r can be calculated from following equations:

$$c_m = \frac{N_m}{N_m + N_l + N_r}, \quad c_l = \frac{N_l}{N_m + N_l + N_r}, \quad c_r = \frac{N_r}{N_m + N_l + N_r}$$

where, N_m, N_l and N_r can be accurately measured. However, accurately measurement and calibration on a physical 3-D display device takes significant effort–it is tedious and error-prone. Furthermore, there are variety ways for the perspective zone's edge intersects with the boundary of the subpixel. It is fairly tricky work to calculate and calibrate the viewable areas for all pixels.

To solve these long-standing problems, we propose a new optimization for crosstalk reduction based on a light field framework. When crosstalk is present in a stereoscopic display, light from one image channel leaks into another, which deteriorates image quality and generates ghosted image. We have investigated the causes for the leakage of unintended lights. When the viewer observes from one viewing position, they will see the corresponding view as if the view image is displayed on the lenticular sheet, with the resolution of $H \times W$. We apply the back projection method with subpixel resolution (each pixel is composed of R, G and B subpixels). A practical implementation strategy of light field 3-D display is to take a subsample of continuously distributed light field function and $n \times H \times W \times 3$ rays approximate the continuous n-view light field. The key issue is to determine the points where the rays emit from the LCD panel. We apply a ray back projection method, which traces the pixel in the view images to the LCD screen. There are also forward projection methods which trace the ray originated from the LCD to determine its color by interpolating the light field [23][24]. The technique of ray back projection method is capable of producing a very high degree of visual realism, for it generates an image by tracing the path of light through pixels in an image plane and simulating the effects of its encounters with optical lens. The ultimate goal of 3-D display systems is to reproduce the target light field as if the images were put in the front of the lenticular sheet for the different viewing positions. Specifically, our contributions include:

1) A novel light field decomposition method for mapping. All the rays of the multiview light field are back projected to the LCD plane along the optical path to form a synthetic image;
2) Our proposed ray mergence and assignment method reduces viewer discomfort for the high contrast region. Weighted values are assigned for each subpixel considering all rays from a dominant and a non-dominant view. Rays from the views mix, providing a weighted-value, $V_d(i,j)$ or $V_{nd}(i,j)$ for the dominant or non-dominant view, respectively, for a subpixel. For each subpixel, (i,j), the dominate $(W_d(i,j))$ and non-dominate $(W_{nd}(i,j))$ view weights are set to correct and optimize the final sum, $S(i,j) = W_d(i,j) + W_{nd}(i,j)$. $S(i,j)$ ensures an upper bound of 255 for the subpixel and a smooth fusion of the two views. Hence, the perception of crosstalk (ghosting) decreases significantly. Compared with the common crosstalk coefficients calculation method, our proposed method is simple and effective.
3) Since our method smoothly integrates rays from different views, crosstalk at any observation position can be reduced compared to other methods.

II. Method Overview

A schematic of the proposed light field technique is shown in Fig. 2. First, the view images are up-sampled from 360×640 to 1080×1920 to simulate the discrete light field. When viewers observe from the n-th viewing position, they will see the n-th view light field emitting from the lenticular sheet as if the up-sampled n-view image were placed on the sheet. Any 9-view light field emitted by the lenticular display can be represented by $9 \times 1080 \times 1920 \times 3$ rays. For a given ray, we determine the intersection point, (x, y), with the lenticular sheet and the transmission angle, δ. Each ray is mapped back along the optical path to its emitting point. A ray mergence and assignment method is introduced to provide crosstalk reduction and smooth fusion of different views. We conducted experiments using a lenticular sheet and an LCD screen, as listed in Table I.

III. Light Field Decomposition

In this part, each ray of multiview light field is back-projected to the LCD plane to form a synthetic image, with subpixel resolution. After the light field decomposition, each ray will be traced back to a emitting point, (x', y'), on the LCD plane.

Stereoscopic 3-D displays present a 3-D image to an observer by sending a light field of slightly different perspective view to each eye, as shown in Fig. 2(b). Consider the light field of

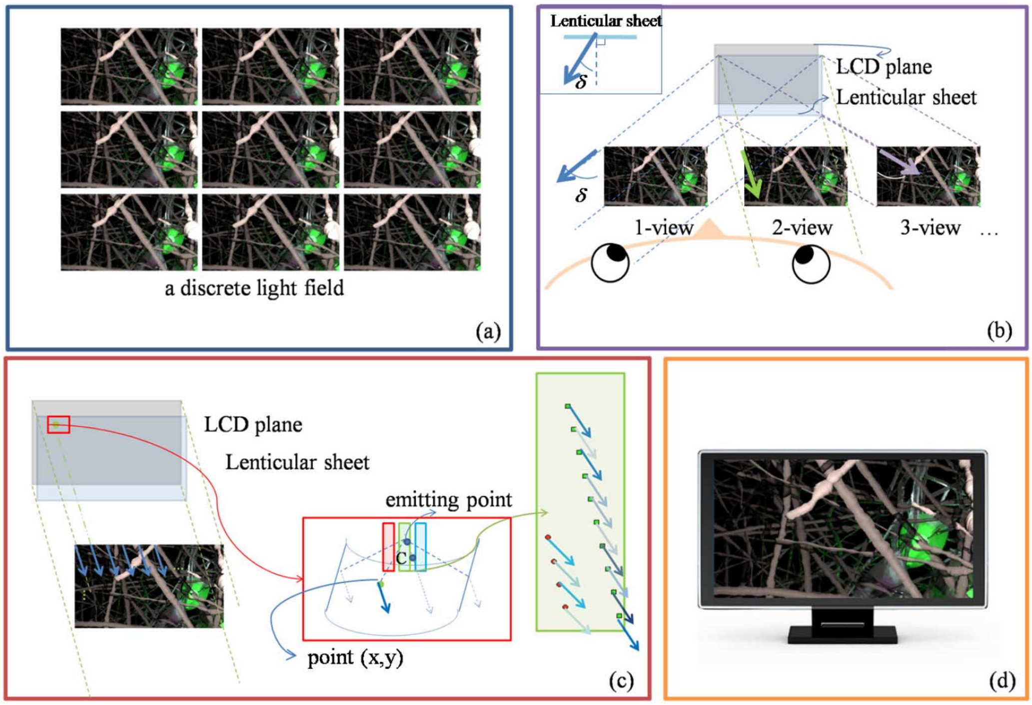

Fig. 2. Overview of our proposed light field decomposition method. (a) Nine input view images are up-sampled to represent the 9-view light fieldemitted by the lenticular display. (b) Ray transmission angle,, is calculated and the intersection (x, y) with the lenticular sheet is pre-defined. (c) Rays are mapped back to the LCD plane following the optical path. Multiple rays may be mapped to one subpixel. A weighted value considering all arriving rays is assigned for the subpixel. A smooth fusion of different views is obtained after ray mergence and assignment. (d) The final synthetic image is generated.

TABLE I
PARAMETERS OF THE 3-D LENTICULAR DISPLAY IN OUR EXPERIMENT

Parameters	Specification
LCD size	21.5'
LCD resolution (H × W)	1080×1920
Multiview image resolution	360×640
Lenticular lens per inch	30.15
Slant angle α	15.524°
View number	9

1-view [Fig. 2(b)], it completely characterizes all the rays generated by the lenticular sheet when the viewer observes from the 1-viewing position. Each ray can be traced back to a subpixel on the LCD panel. If all the observable subpixels are illumined with color and the other subpixels are set to be transparent, the 1-view image will be observed through the lenticular sheet at its viewing position. The RGB arrangement on the LCD panel is standard, and so subpixels on the LCD panel have the same physical location as subpixels on the synthetic image. Hence, if we utilize the task from 2–9-views, the final synthetic image will be generated on the LCD panel.

In the back-projection procedure, each subpixel on the LCD plane receives rays partly from one view and partly from a neighboring view. We consider these rays from two views and calculate the subpixel values (see details in Section IV).

For a 9-view display, each lenticular lens is equally divided into 9 perspective zones [21], [22]. The zone on the lenticular sheet illuminated with yellow and green color in Fig. 3. is prepared for the observer at the 4th and 3rd optimal viewing position respectively. Blue lines represent the edges of perspective

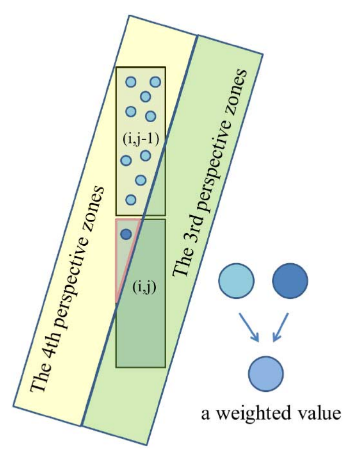

Fig. 3. Light from third image channel leaking into the fourth channel. The weighted value considers all rays from the two views assigned for the (i, j)-subpixel, reducing the effect.

zones. If we set the (i, j)-subpixel with the color of the 3-view image's subpixel, a few rays from 3-view image (marked with red triangle) will be observed through the lenticular sheet at the 4-view position, which causes crosstalk. If we combine the color from the two views to determine the value of (i, j)-subpixel, less rays of the 3-view image's color will leak into the 4-view position. The key to this problem is to determine the weighted value and ensure smooth fusion of different views.

A 3-D lenticular display consists of a lenticular sheet and a LCD panel. The lenticular sheet is composed of an array of slanted cylindrical lenses. Subpixels are located at the focal

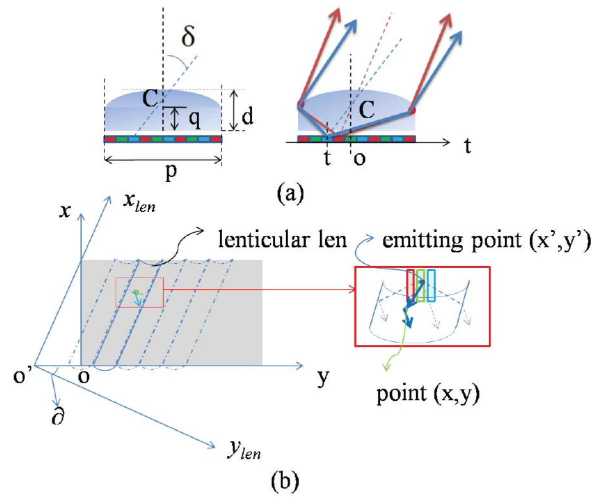

Fig. 4. (a) Structure of cylindrical lens. (b) Following the optical path, the emitting point, (x', y'), on the LCD plane is available.

plane of the cylindrical lenses. As shown in Fig. 4(a)., C represents the panel point of the cylindrical lens, p is the lens width, and q is the distance between C and the focal plane. When the rays from a point on the t axis spreads through the cylindrical lens, they becomes parallel. The transmission angle, δ, is

$$\begin{cases} \delta = 0^\circ, & if\ t = 0 \\ \delta = arctan\left(\frac{t}{q}\right), & if\ t \neq 0 \end{cases} \tag{1}$$

A ray of the light field is shown in Fig. 4(b)., where (x, y) is the coordinate where the ray passes through the lenticular sheet. The coordinate systems of the lenticular sheet and the LCD plane are $\mathrm{x_{len}o'y_{len}}$ and xoy respectively.

We refer to the pose of $\mathrm{x_{len}o'y_{len}}$ with respect to the LCD plane frame of reference xoy as:

$$\mathrm{T_{Ll}} = \begin{pmatrix} \cos\alpha & \sin\alpha & -\mathrm{Hdispaly} \\ -\sin\alpha & \cos\alpha & 0 \\ 0 & 0 & 1 \end{pmatrix} \tag{2}$$

where $\mathrm{T_{Ll}}$ is the matrix describing point transfer between the lenticular sheet's frame and that of the LCD plane. α is the slant angle of lenticular sheet.

The point (x, y) is transformed from xoy to $\mathrm{x_{len}o'y_{len}}$ as a point $(\mathrm{x_{len}}, \mathrm{y_{len}})$:

$$\begin{pmatrix} \mathrm{x_{len}} \\ \mathrm{y_{len}} \\ 1 \end{pmatrix} = \mathrm{T_{Ll}}^{-1} \begin{pmatrix} \mathrm{x} \\ \mathrm{y} \\ 1 \end{pmatrix} \tag{3}$$

According to the Eq. (1), the emitting point (a, b) in the lenticular sheet's frame can be calculated as:

$$\begin{cases} a = \lceil \mathrm{x_{len}}/\mathrm{p} \rceil \times \mathrm{p} + \mathrm{q}\tan\delta \\ b = y_{len} \end{cases} \tag{4}$$

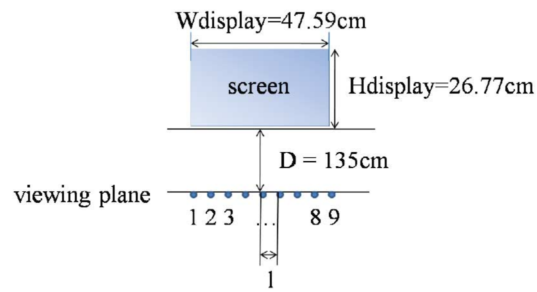

Fig. 5. Structure of a viewing system.

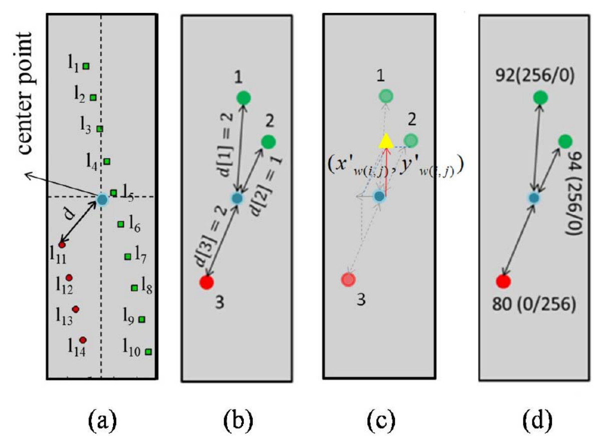

Fig. 6. (a) Several rays from light field may be back-projected to the same subpixel. The red points represent rays from the $\mathrm{n}+1$ view and green points the n-th view. Most green points have the same value, except for high contrast regions. (b) The final value, L, is set for the subpixel and replaces the original ray values to generate a light filed. The goal is to find a reasonable L value to simulate the target light field. (c) The example for w[k]'s calculation. (d) The example for calculation of $\mathrm{W_d}$, $\mathrm{W_{nd}}$ and the final value L, with the assumption that $\mathrm{j} = 6 \mathrm{and} \mathrm{j'} = 1$.

The emitting point, $(\mathrm{x'}, \mathrm{y'})$, where the light will be traced back to the LCD plane is

$$\begin{pmatrix} \mathrm{x'} \\ \mathrm{y'} \\ 1 \end{pmatrix} = \mathrm{T_{Ll}} \begin{pmatrix} \mathrm{a} \\ \mathrm{b} \\ 1 \end{pmatrix} \tag{5}$$

Rays from one view have the same transmission angle, estimated from $\delta = arctan((n-5) \times l/D)$, where n is the number of the view image, l is the distance between two neighboring viewing positions, and D is the viewing distance as shown in Fig. 5.

IV. Ray Mergence and Assignment

In this part, we introduce a ray mergence and assignment to provide crosstalk reduction and smooth fusion of different views, which performs the following two-stage procedure:

- For each subpixel, we calculate two weighted-value, $V_d(i,j)$ and $V_{nd}(i,j)$, for the rays from dominant and non-dominant view.
- For each subpixel, we calculate the $W_d(i,j)$ and $W_{nd}(i,j)$ to correct and optimize the final sum $L(i,j)$.

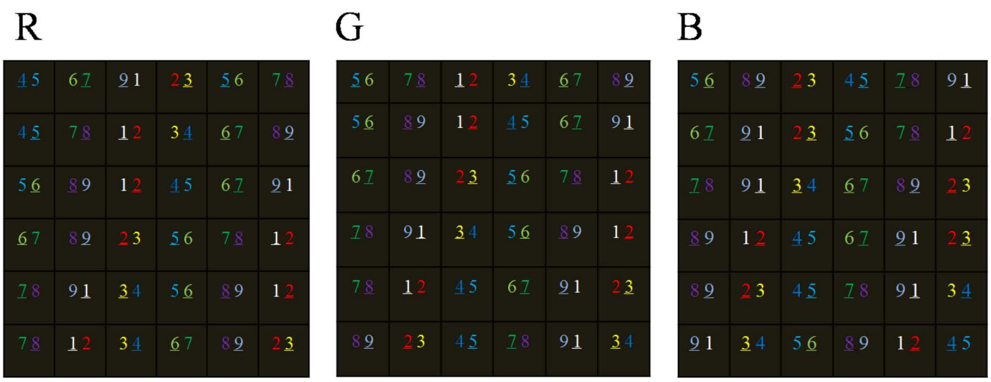

Fig. 7. Due to the hardware constraint for our lenticular sheet, only two views' rays reach any subpixel and we call the two views' rays a ray pair. The figure shows each ray pair is combined two neighboring views for each point on the R, G, or B maps. The dominant view is noted by underline. We set a sum-weight for each subpixel on the LCD plane to limit the view fusion.

(1) Calculation of $V_d(i,j)$ and $V_{nd}(i,j)$: Several rays from the light field may be projected to a same subpixel during the ray-back projection process, as shown in Fig. 6(a). The emitting point of each ray, $(\mathrm{x}', \mathrm{y}')$, is belonging to a subpixel on the LCD plane. The distance, $d[k]$, from the $(\mathrm{x}', \mathrm{y}')$ to the center of this subpixel cane calculated. The weighted value V of the (i, j) subpixel is

$$V\left(i,j\right) = \sum\nolimits_{k=1}^{n} l[k] \times w[k] \; and \; w[k] = \frac{1}{d[k]} \bigg/ \sum\nolimits_{t=1}^{n} \frac{1}{d[t]}\,, \tag{6}$$

where n is the number of the rays, $l[k]$ is the light intensity of the k-th ray. A reasonable assumption is that the ray emitting nearer to the center point of the subpixel has a larger weight term w. So the $w[k]$ is inversely proportional to $d[k]$. Take Fig. 6(b). for simplicity, the d for 1-3 points are 2, 1, 2, so the $w[1] = 0.25(= (\frac{1}{2})/(1+\frac{1}{2}+\frac{1}{2}))$, $w[2] = 0.5$, $w[3] = 0.25$. The yellow triangle shown in Fig. 6(c) represents the virtual emitting point $(x'_{w(i,j)}, y'_{w(i,j)})$ with weighted value $V(i,j)$, and the corresponding position are calculated by a weighed eigenvector arithmetic.

Due to the hardware constraint for our lenticular sheet, only two views' rays reach any subpixel. For simplicity, we assume that n-th view image (green point) is the dominate view and n+1-th view image (red point) is the non-dominate view for the (i, j) subpixel hereinafter. Each subpixel of the synthetic image combines a pair of rays from neighboring view images, the dominate view and non-dominate view. Eq. (6) can be expressed as

$$V\left(i,j\right) = V_d\left(i,j\right) + V_{nd}\left(i,j\right), \tag{7}$$

where

$$V_d\left(i,j\right) = \sum\nolimits_{k1=1}^{n1} l\left[k1\right] \times w\left[k1\right] \tag{8}$$

$$V_{nd}\left(i,j\right) = \sum\nolimits_{k2=n1+1}^{n} l\left[k2\right] \times w\left[k2\right] \tag{9}$$

and $n1$ is the number of the rays from dominate view. The rays mapped from one view usually come from an adjacent area on the view image. In most cases, the ray color remains constant. However, for marginal (high-contrast) regions, the sharp change of color causes viewer discomfort and reduced image quality. But our proposed method weighting the coming rays effectively smoothes the variation, and the perception of crosstalk (ghosting) decreases significantly.

(2) Calculation of $W_d(i,j)$ and $W_{nd}(i,j)$: However, the subpixel value $V(i,j)$ on the final synthetic image may exceed 255 after mapping the view images. To reproduce a reasonable light field on a high contrast display and a smooth fusion of views, we set W_d and W_{nd} to limit the maximum value of the (i,j) subpixel. The final value:,

$$L\left(i,j\right) = W_d\left(i,j\right) \times V_d\left(i,j\right) + W_{nd}\left(i,j\right) \times V_{nd}\left(i,j\right), \tag{10}$$

where $W_d(i,j)$ and $W_{nd}(i,j)$ are obtained explicitly below:

The n-th view image is set with white color (255), and the other view images are set to black (0). That is, the red points from the $\mathrm{n}+1$ view image are set value 0 in Fig. 6(a), and the green points from the n-th view image are set to 255. We get a dominant weighted value, $\mathrm{V_{d255}}$, from Eq. (8). Similarly, a non-dominant weighted value, $\mathrm{V_{nd255}}$, is calculated when the $\mathrm{n}+1$ view image is white and the other view images are set to be black.

For each (i,j) subpixel, $S(i,j) = W_d(i,j) + W_{nd}(i,j)$ to ensure a smooth fusion of views and a maximum value of 255 for each subpixel (see results in Section V). W_d and W_{nd} are calculated as:

$$W_d = S\left(i,j\right) \times \frac{V_{d255}}{V_{d255} + V_{nd255}} \tag{11}$$

$$W_{nd} = S\left(i,j\right) \times \frac{V_{nd255}}{V_{d255} + V_{nd255}} \tag{12}$$

and (13), shown at the bottom of the following page, where

$$j' = \left\lceil \frac{x_{w(i,j)}}{\mathrm{Wdispaly}} \times \mathrm{W}' \right\rceil$$

$\mathrm{W}' \times \mathrm{H}'$ is the resolution of the view image. and $x_{w(i,j)}$ is the horizontal coordinate of the point where the ray passes through the lenticular sheet from virtual emitting point $(x'_{w(i,j)}, y'_{w(i,j)})$. The $x_{w(i,j)}$ can be calculated through the inverse operation of the back projection. In Fig. 6(d). for example, we obtained the final value as following:

$$V_{d255} = \sum_{k=1}^{2} 255 \times w[k] = 0.5 \times 255 + 0.25 \times 255 = 192,$$

$$V_{nd255} = \sum_{k=1+2}^{3} 255 \times w[k] = 0.25 \times 255 = 64,$$

and assuming $j = 6 \quad and \quad j' = 1$, then

$$W_d = S(i,j) \times \frac{V_{d255}}{V_{d255} + V_{nd255}} = \frac{213}{255} \times \frac{192}{255} = 0.624,$$

$$W_{nd} = S(i,j) \times \frac{V_{nd255}}{V_{d255} + V_{nd255}} = \frac{213}{255} \times \frac{64}{255} = 0.208,$$

So

$$V_{d255} = \sum_{k=1}^{2} l[k] \times w[k] = 0.25 \times 92 + 0.5 \times 94 = 70,$$

$$V_{nd255} = \sum_{k=1+2}^{3} l[k] \times w[k] = 20,$$

and since $L = W_d \times V_d + W_{nd} \times V_{nd}$,

$$L = 0.624 \times 70 + 0.208 \times 20 = 47.84.$$

V. Results and Discussion

(1) Crosstalk Reduction Measurement: Compared with the crosstalk coefficients calculation method, the proposed method is able to reduce the crosstalk effectively, especially the point between two observation perspective.

A camera array with pitch of 2.46 cm was moved horizontally to measure the intensity in a range of viewing position, simulating a person moving from side to side, at a pre-determined viewing distance. We obtained nine black-and-white test images by lighting each view image in turn on the display screen. For these tests, only subpixels corresponding to a certain view image were turned on at maximal intensity and all other subpixels were turned off. Then, we measured each captured image's intensity, respectively, along the horizontal direction. In our test, camera array was moved only 2.46 cm in horizontal direction and about every 0.615 cm captured a group of images (9 images in each group). Fig. 8(a) and 8(b) show the optical output of a lenticular multiview auto stereoscopic display without and with crosstalk reduction, respectively.

The relative luminance of each view is shown for a selection of observation positions [Fig. 8(a)]. When the second view reaches maximum intensity at the second observation perspective, the luminance of the third view is approximately 0.25 and the first view is approximately 0.15, which causes crosstalk. However, our proposed method reduces the intensity of the third view to 0.06 and the first view to 0.01. Compared with the common crosstalk coefficients calculation method [Fig. 8(c)], our proposed method also reduce the crosstalk between two

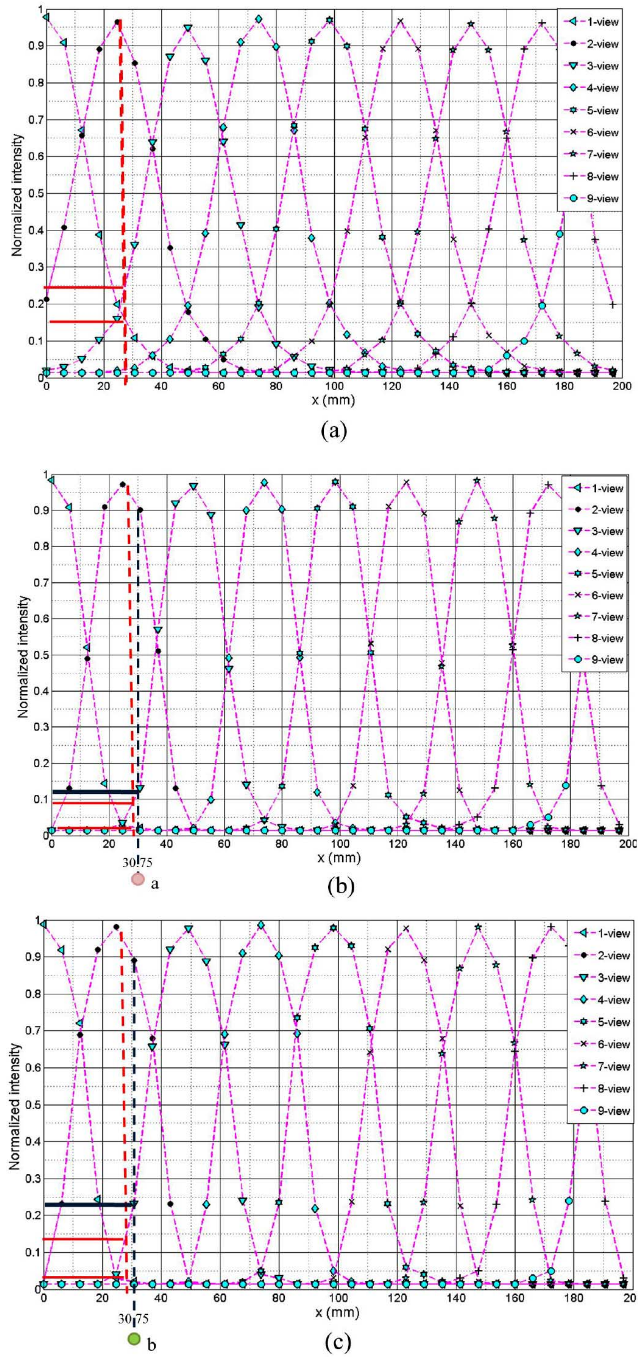

Fig. 8. Visibility of different perspective views for an example lenticular multiview auto stereoscopic display when viewed from different horizontally spaced observation points. (a) Without crosstalk reduction. (b) With crosstalk reduction using our proposed method. (c) With crosstalk reduction using the crosstalk coefficients calculation method.

$$S(i,j) = \begin{cases} \frac{43}{255}, & if \ \left\lfloor \frac{j}{3} \right\rfloor = (j'-1) \times 3 \ or \ j = (j'-1) \times 3 + 5 \\ \frac{127.5}{255}, & if \ \left\lfloor \frac{j}{3} \right\rfloor = (j'-1) \times 3 + 1 \ or \ j = (j'-1) \times 3 + 4 \\ \frac{212}{255}, & if \ \left\lfloor \frac{j}{3} \right\rfloor = (j'-1) \times 3 + 2 \ or \ j = (j'-1) \times 3 + 3 \end{cases}, \tag{13}$$

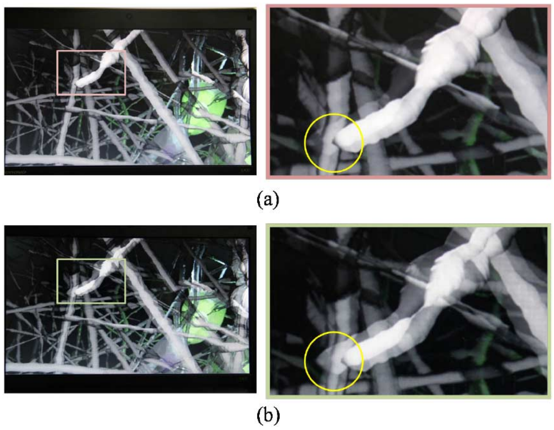

Fig. 9. Views captured at (a) point a. (b) point b.

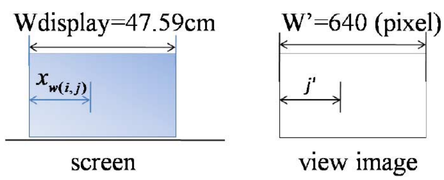

Fig. 10. j' can be regarded as the column coordinate of a given pixel on the view image.

observation perspective. For example, from viewing position 30.75, the intensity sum from view 2 and 3 is almost 1. We captured the view image at points a and b and, as shown in Fig. 9, our proposed method reduces zone jumping between observation points because of the smooth fusion of different views, which also disguises crosstalk.

(2) Smooth Fusion of Different Views: After the a ray mergence and assignment, integrated lights from neighboring views well at all observation positions across the display from a range of viewing positions.

For simplicity, j' in Eq. (13) can be regarded as the column coordinate of a given pixel on the view image from the perspective of the physical location (Fig. 10). In the test, only the pixels of column $j' \in [1, 640]$ on the first view image are set white, and the other pixels are set black. When rays are mapped back to LCD plane against the optical path, the pixels on the synthetic image ranging from the $t(j' - 1) \times 3$ to $(j' - 1) \times 3 + 5$ columns receive rays. We perform this for 2–9-views respectively, and the pixel values on the synthetic image are shown in Fig. 11(a). Fig. 11(b) shows the case when we apply the task to from 1 to n view ($n = 2, 3, 4, \cdots, 9$). The result in (b) is equal to a superposition of corresponding views in (a). For example, if we add views 1 to 6 pattern in (a), we obtain the 6th pattern in (b). After limiting the subpixel maximums, a smooth fusion of different views is achieved.

Consider the last pattern in Fig. 11(b). If pixels of the $j' - 1$ and $j' + 1$ columns are also illuminated white on all the view images, the pixels on synthetic image from columns $(j' - 2) \times 3$ to $(j' - 2) \times 3 + 5$ and $j' \times 3$ to $j' \times 3 + 5$ columns will be assigned. As shown in Fig. 12, all these lighted pixels are able to be smoothly integrated. If we set all view images with white color, the pixel values on the synthetic image will be exactly

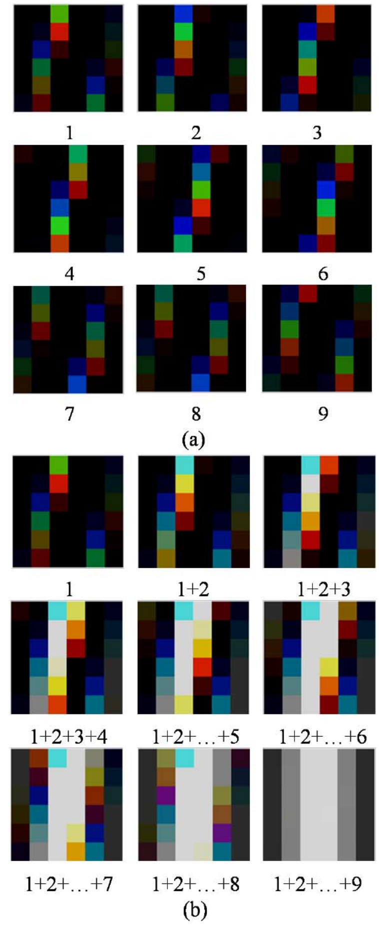

Fig. 11. Smooth fusion of different views is achieved. The coordinate of a given pixel on the view image is (i', j'). Consider the example of the pixels in a pattern on the synthetic image. (a) Column j' column pixels set to white on each view image. (b) Applying the proposed method to views 1 to n.

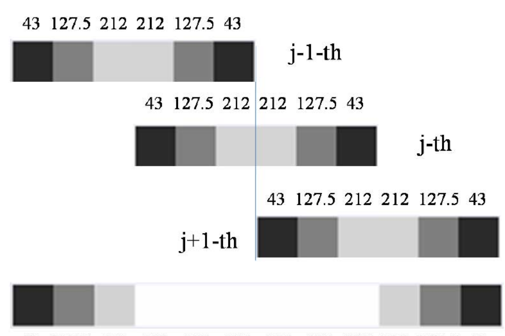

Fig. 12. Taking a single row as an example, we set the pixels in columns $j' - 1$ to $j' + 1$ to be white, producing the synthetic image marked with the blue rectangle.

255 after the mapping. Thus, the proposed method provides a smooth fusion of different views.

(3) Optimization Method Comparison: We implemented the proposed approach in C/C++ platform with an Intel(R) Core(TM) i7-4770 K CPU@3.50 GHz (8 CPUs), 3.5 GHz. The whole proposed method costs 18.56s for a 1920 × 1080 synthetic image. However, the crosstalk coefficients calculation method costs about 29.71 s. Table II compares the outcomes for the 3-D lenticular display reduction system. Our proposed

TABLE II
RESULTS COMPARING

Method	Advantage	Disadvantage
Parallax values decrease	Simple	Depth sense decline; Crosstalk doesn't reduced substantially
Aperture ratio decrease	Simple	Applying only to parallax barrier type display; Sacrificing the intensity
Timing control	Effective	Requiring extra devices
Crosstalk coefficients calculation	Effective; Without extra devices	Requiring significant effort on alignment and the viewable areas' calculation; The crosstalk between two observation perspective still remains
Our method	Simple, effective and low-cost; The crosstalk between two observation perspective is also reduced effectively; A smooth fusion of different views is achieved; Without extra devices	Parameter q should be accurately calibration on physical device

method, based on the light field, is simple, effective, and low-cost.

VI. CONCLUSION

We proposed a novel crosstalk reduction method based on light field analysis. We developed a ray mergence and assignment method that reduced viewer discomfort on high contrast regions, based on optimization of light field generated by the lenticular 3-D display. The perception of crosstalk (ghosting) decreases significantly, and the smooth fusion of different views further disguises crosstalk. Experimental results validate that our proposed method reduces crosstalk and is simple, effective, and low-cost. In further work, we intend to accelerate our algorithms by utilizing the GPU.

REFERENCES

[1] J. Geng, "Three-dimensional display technologies," *Adv. Opt. Photon.*, vol. 5, no. 4, pp. 456–535, 2013.
[2] Y. Fan, Y. Kung, and B. Lin, "Three-dimensional auto-stereoscopic image recording, mapping and synthesis system for multiview 3D display," *IEEE Trans. Magn.*, vol. 47, no. 3, pp. 683–686, Mar. 2011.
[3] C. van Berkel, "Image preparation for 3D-LCD," in *Proc. SPIE 3639, Stereoscopic Displays and Virtual Reality Systems VI*, May 24, 1999, vol. 84.
[4] M. Levoy and P. Hanrahan, "Light field rendering," in *Proc. 23rd Annu. Conf. Comput. Graphics and Interactive Techn.*, 1996, pp. 31–42.
[5] A. Jones, I. McDowall, H. Yamada, M. Bolas, and P. Debevec, "Renderingfor an interactive 360° light field display," presented at the SIGGRAPH, 2007, paper 40.
[6] G. Wetzstein, D. Lanman, W. Heidrich, and R. Raskar, "2011 Layered 3D: Tomographic image synthesis forattenuation-based light field and high dynamic range displays," *ACM Trans. Graph.*, vol. 30, no. 4, p. 11, Jul. 2011, Art. ID 95.
[7] D. Lanman, G. Wetzstein, M. Hirsch, W. Heidrich, and R. Raskar, "Polarization fields: Dynamic light field display using multi-layer LCDs," *Trans. Graphics ACM SIGGRAPH Asia*, vol. 30, no. 6, 2011, Art. ID 95.
[8] X. Cao, J. Geng, and T. Li, "Dictionary-based light field acquisition using sparse camera array," *Opt. Exp.*, vol. 22, no. 20, pp. 24081–24095, 2014.
[9] L. Xing, J. You, T. Ebrahimi, and A. Perkis, "Assessment of stereoscopic crosstalk perception," *IEEE Trans. Multimedia*, vol. 14, no. 2, pp. 326–337, Apr. 2012.
[10] A. J. Woods, "Crosstalk in stereoscopic displays: A review," *J. Electron. Imaging*, vol. 21, no. 4, Oct.–Dec. 2012, Art. ID 040902.
[11] X. Li, Q. Wang, D. Li, and A. Wang, "Image processing to eliminate crosstalk between neighboring view images in three-dimensional lenticular display," *J. Display Technol.*, vol. 7, no. 8, pp. 443–447, Aug. 2011.
[12] H. Liao, MIwahara, NHata, and TDohi, "High quality integral videography by using a multi-projector," *Opt. Exp.*, vol. 12, no. 6, pp. 1067–1076, 2004.
[13] TOkoshi, *3 Dimensional Imaging Techniques*. New York, NY, USA: Academic, 1976, ch. 2, pp. 8–42.
[14] TNagoya, TKozakai, TSuzuki, MFuruya, and KIwase, "The D-ILA device for the world's highest definition (8K4 K) projection systems," in *Proc. IDW*, 2008, pp. 203–206.
[15] YKusakabe, MKanazawa, YNojiri, MFuruya, and MYoshimura, "A high dynamic range and high resolution projector with dual modulation," in *Proc. SPIE 7241*, 2009, pp. 72410Q–72410Q-11.
[16] YTao, QWang, JGu, WZhao, and DLi, "Autostereoscopic three-dimensional projector based on two parallax barriers," *Opt. Lett.*, vol. 34, no. 20, pp. 3220–3222, 2009.
[17] CLee, GSeo, JLee, THan, and JPark, "Auto-stereoscopic 3D displays with reduced crosstalk," *Opt. Exp.*, vol. 19, no. 24, pp. 24762–24774, 2011.
[18] WZhao, QWang, AWang, and DLi, "Autostereoscopic display based on two-layer lenticularlenses," *Opt. Lett.*, vol. 35, no. 24, pp. 4127–4129, 2010.
[19] M. Salmimaa and T. Järvenpää, "3D crosstalk and luminance uniformity from angular luminance profiles of multi-view autostereoscopic3-D displays," *J. Soc. Inf. Display*, vol. 16, pp. 1033–1040, 2008.
[20] T. H. Hsu, M. H. Kuo, H. H. Huang, S. C. Chang, and C. H. Chen, "High resolution autostereoscopic 3-D display with proximity projectorarray," in *Proc. SID*, 2008, pp. 760–763.
[21] X. Wang and C. Hou, "Improved crosstalk reduction on multiview 3D display by using BILS algorithm," *J. Appl. Math.*, vol. 2014, Art. ID 428602.
[22] B. A. Olshausen and B. J. Field, "Sparse coding with an overcomplete basis set: A strategy employed by v1," *Vis. Res.*, vol. 37, pp. 3311–3325, 1997.
[23] J. Wang, H. Suenaga, H. Liao, K. Hoshi, L. Yang, E. Kobayashi, and I. Sakuma, "Real-time computer-generated integral imaging and 3D image calibration for augmented reality surgical navigation," *Computerized Medical Imaging and Graphics*, vol. 40, no. 2015, pp. 147–159.
[24] G. Wetzstein, D. Lanman, M. Hirsch, and R. Raskar, "Tensor displays: Compressive light field synthesis using multilayer displays with directional backlighting," presented at the SIGGRAPH, 2012.

Renjing Pei is currently working toward the Ph.D. degree in control theory and control engineering at the institute of automation, Chinese Academy of Sciences, Beijing, China. Her research interests are 3-D display and 3-D reconstruction.

Jason Geng received the Ph.D. degree in electrical engineering from George Washington University in 1990. Since then, he has led a variety of research, development, and commercialization efforts on 3-D imaging technologies. He founded a high tech company that specialized in developing 3-D imaging technologies and products. He has served as a principal investigator and major contributor for over $35 million in research and product efforts. He has published 142 academic papers and one book and is an inventor of 33 issued patents.

Dr. Geng currently serves as the vice president for the IEEE Intelligent Transportation Systems Society (ITSS). He is also leading Intelligent Transportation System standard efforts by serving as the chairman of the standard committee for IEEE ITSS. His recent publication on 3-D imaging

technology ("Structured light 3-D surface imaging: a tutorial,"www.opticsinfobase.org/aop/abstract.cfm?uri=aop-3?2?128) was among the top downloaded articles in the OSA Advances in Optics and Photonics (AOP) journal. He has received prestigious national honors, including the Tibbetts Award from the U.S. Small Business Administration and the "Scientist Helping America" award from the Defense Advanced Research Projects Agency, and was ranked 257 in INC. magazine's "INC. 500 List."

Zhao Xing Zhang received the B.S. degree in opto-electronic information engineering and M.S. degree in bio-medical engineering from Nanjing University of Science and Technology in 2007 and 2009, respectively. As an engineer in the Institute of Automation, Chinese Academy of Sciences (CASIA) since 2008, his current research includes the 3-D reconstruction, true 3-D display and other relative areas. He has also published several papers at the SPIE/IST conference and held several patents in these areas.

Xuan Cao received the B.S. degree in electric engineering from Harbin Institute of Technology, China. He is currently working toward the Ph.D. degree at the Computer Science at Chinese Academy of Sciences. His study of interests is 3-D displays and computational photography. He worked as an intern at the ICT Graphics Lab, USC.

Rong Wang received the B.S. degree in automation from Beihang University, China, in 2013. She is currently working toward the Ph.D. degree at the of Automation of Chinese Academy of Sciences. Her research interests include 3-D surface registration, reconstruction and augmented reality visualization.